

DEVELOPMENT OF EFFICIENT GEOMETRIC MULTIGRID ALGORITHMS BY LFA FOR SYSTEMS OF PARTIAL DIFFERENTIAL EQUATIONS ON TRIANGULAR GRIDS

F. J. Gaspar, J. L. Gracia, F. J. Lisbona and C. Rodrigo

Abstract. In this paper Local Fourier Analysis (LFA) for multigrid methods on triangular grids is extended to the case of systems of PDEs. In particular, it is performed for the problem of planar elasticity, although its application to other systems is straightforward. Analogously to the scalar case, this analysis is based on an expression of the Fourier transform in new coordinate systems, both in space and in frequency variables, associated with reciprocal bases. LFA is particularly valuable for systems of PDEs, since it is often much more difficult to identify the correct multigrid components than for a scalar problem. For the discrete elasticity operator obtained with linear finite elements, different collective smoothers like three-color smoother and some zebra-type smoothers are analyzed. LFA results for these smoothers are presented.

Keywords: Geometric multigrid, Fourier analysis, three-color smoother, triangular grids, elasticity.

AMS classification: 65N55, 65F10, 65N30.

§1. Introduction

Planar elasticity models the displacements of an elastic body $\Omega \subset \mathbb{R}^2$, subject to a force density \mathbf{f} , with respect to its original configuration. These displacements are described by means of a vector function $\mathbf{u} = (u, v)$, which is the solution of the following system of equations

$$\mathbf{L} \mathbf{u} = -\mu \Delta \mathbf{u} - (\lambda + \mu) \text{grad}(\text{div} \mathbf{u}) = \mathbf{f}, \quad \text{in } \Omega,$$

where Δ is the vector Laplace operator, λ and μ are the so-called Lamè's coefficients, and $\mathbf{f} = (f_1, f_2) \in (L^2(\Omega))^2$. Here, a discretization by linear finite elements of this elasticity operator is considered,

$$\mathbf{L}_h = \begin{pmatrix} L_h^{u,u} & L_h^{u,v} \\ L_h^{v,u} & L_h^{v,v} \end{pmatrix} = \begin{pmatrix} -(\lambda + 2\mu)(\partial_{xx})_h - \mu(\partial_{yy})_h & -(\lambda + \mu)(\partial_{xy})_h \\ -(\lambda + \mu)(\partial_{xy})_h & -\mu(\partial_{xx})_h - (\lambda + 2\mu)(\partial_{yy})_h \end{pmatrix}.$$

The algebraic linear equation system arising from this discretization will be solved by means of a geometric multigrid algorithm, due to the fact that these methods are among the most efficient numerical algorithms for solving this kind of systems. In geometric multigrid, a

hierarchy of grids must be proposed. For an irregular domain, it is very common to apply regular refinement to an unstructured input grid; in this way, a hierarchy of globally unstructured grids is generated that is suitable for use with geometric multigrid. So, we are interested in the framework of hierarchical hybrid grids (HHG) which was presented in [1]. The coarsest mesh is assumed rough enough in order to fit the geometry of the domain. Once this coarse triangulation is given, each triangle is divided into four congruent triangles connecting the midpoints of their edges, and so forth until the mesh has the desired fine scale to approximate the solution of the problem. In this way, a nested hierarchy of grids is obtained.

As it is well-known, the construction of an efficient multigrid method is strongly dependent on the choice of its components, which have to be selected so that they efficiently interplay with each other. Especially, the choice of a suitable smoother is an important feature for the design of an efficient multigrid method. In this paper, linear interpolation has been chosen, the restriction operator has been taken as its adjoint and the discrete operator corresponding to each mesh results from the direct discretization of the problem. Moreover, collective three-color smoother and some collective line-wise smoothers of zebra-type are proposed as relaxing methods.

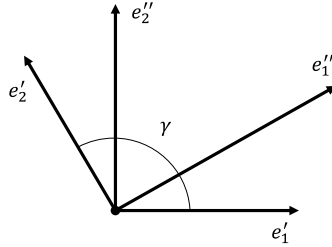
In order to choose suitable components for a multigrid method, LFA is used, due to its being a powerful tool for the design of efficient multigrid methods. This analysis is mainly based on the Fourier transform and was introduced by Brandt [2]. A good introduction can be found in the books by Trottenberg et al. [4] and Wienands and Joppich [5]. This technique has been widely used in the framework of discretizations on rectangular grids, and recently a generalization to triangular grids has been proposed in [3]. The key fact for carrying out this generalization is to write the Fourier transform using coordinates in non-orthogonal bases fitting the new structure of the grid. In order to extend LFA to the case of the planar elasticity system, a new expression of the Fourier transform for vector functions is considered. To study multigrid methods in the framework of HHG, the LFA proposed here is applied to each input triangle in such a way that the global behavior of the method will depend on the quality of the chosen local components.

The organization of the paper is as follows. In Section 2, the way in which LFA can be performed on non-orthogonal grids for systems of PDEs is explained. In section 3, the relaxation methods considered, three-color and zebra-type smoothers are presented. Finally, in Section 4, some LFA results are shown in order to choose the relaxation method of the multigrid algorithm which is more suitable for different grid geometries.

§2. Fourier analysis on non-orthogonal grids

A non-orthogonal unitary basis of \mathbb{R}^2 is established: $\{\mathbf{e}'_1, \mathbf{e}'_2\}$ with $0 < \gamma < \pi$ being the angle between the vectors of the basis. It is also considered its reciprocal basis $\{\mathbf{e}''_1, \mathbf{e}''_2\}$, i.e., $(\mathbf{e}'_i, \mathbf{e}''_j) = \delta_{ij}$, $1 \leq i, j \leq 2$, where (\cdot, \cdot) is the usual inner product in \mathbb{R}^2 and δ_{ij} is the Kronecker's delta, see Figure 1. The coordinates of a point in these bases, $\{\mathbf{e}'_1, \mathbf{e}'_2\}$ and $\{\mathbf{e}''_1, \mathbf{e}''_2\}$, are $\mathbf{y}' = (y'_1, y'_2)$ and $\mathbf{y}'' = (y''_1, y''_2)$, respectively, just like $\mathbf{y} = (y_1, y_2)$ in the canonical basis $\{\mathbf{e}_1, \mathbf{e}_2\}$.

By applying the changes of variables $\mathbf{x} = \mathbf{F}(\mathbf{x}')$ and $\boldsymbol{\theta} = \mathbf{G}(\boldsymbol{\theta}')$ to the usual Fourier transform formula, the Fourier transform and its corresponding back transformation formula


 Figure 1: Reciprocal bases in \mathbb{R}^2 .

with coordinates in a non-orthogonal basis, result in the following

$$\begin{aligned}\hat{\mathbf{u}}(\mathbf{G}(\boldsymbol{\theta}'')) &= \frac{\sin \gamma}{2\pi} \int_{\mathbb{R}^2} e^{-i\mathbf{G}(\boldsymbol{\theta}'') \cdot \mathbf{F}(\mathbf{x}')} \mathbf{u}(\mathbf{F}(\mathbf{x}')) \, d\mathbf{x}', \\ \mathbf{u}(\mathbf{F}(\mathbf{x}')) &= \frac{1}{2\pi \sin \gamma} \int_{\mathbb{R}^2} e^{i\mathbf{G}(\boldsymbol{\theta}'') \cdot \mathbf{F}(\mathbf{x}')} \hat{\mathbf{u}}(\mathbf{G}(\boldsymbol{\theta}'')) \, d\boldsymbol{\theta}''.\end{aligned}$$

Since the new bases are reciprocal bases, the inner product $\mathbf{G}(\boldsymbol{\theta}'') \cdot \mathbf{F}(\mathbf{x}')$ is given by $\theta''_1 x'_1 + \theta''_2 x'_2$. Using previous expressions, a discrete Fourier transform for non-rectangular grids can be introduced. With this purpose, a uniform infinite grid is defined:

$$G_h = \{\mathbf{x}' = (x'_1, x'_2) \mid x'_i = k_i h_i, k_i \in \mathbb{Z}, i = 1, 2\},$$

where $\mathbf{h} = (h_1, h_2)$ is a grid spacing. Now, for a vector grid function \mathbf{u}_h , the discrete Fourier transform and its back Fourier transformation can be defined by

$$\begin{aligned}\hat{\mathbf{u}}_h(\boldsymbol{\theta}'') &= \frac{h_1 h_2 \sin \gamma}{2\pi} \sum_{\mathbf{x}' \in G_h} e^{-i(\theta''_1 x'_1 + \theta''_2 x'_2)} \mathbf{u}_h(\mathbf{x}'), \\ \mathbf{u}_h(\mathbf{x}') &= \frac{1}{2\pi \sin \gamma} \int_{\Theta_h} e^{i(\theta''_1 x'_1 + \theta''_2 x'_2)} \hat{\mathbf{u}}_h(\boldsymbol{\theta}'') \, d\boldsymbol{\theta}'',\end{aligned}\tag{1}$$

where $\boldsymbol{\theta}'' = (\theta''_1, \theta''_2) \in \Theta_h = (-\pi/h_1, \pi/h_1] \times (-\pi/h_2, \pi/h_2]$ are the coordinates of the point $\theta''_1 \mathbf{e}'_1 + \theta''_2 \mathbf{e}'_2$ in the frequency space. Considering the scalar Fourier modes, $\varphi_h(\boldsymbol{\theta}'', \mathbf{x}') = e^{i\theta''_1 x'_1} e^{i\theta''_2 x'_2}$, their vector counterparts are $\boldsymbol{\varphi}_h(\boldsymbol{\theta}'', \mathbf{x}') := (\varphi_h(\boldsymbol{\theta}'', \mathbf{x}'), \varphi_h(\boldsymbol{\theta}'', \mathbf{x}'))^t$, with $\mathbf{x}' \in G_h$, and $\boldsymbol{\theta}'' \in \Theta_h$. They give rise to the Fourier space, $\mathcal{F}(G_h) = \text{span}\{\boldsymbol{\varphi}_h(\boldsymbol{\theta}'', \cdot) \mid \boldsymbol{\theta}'' \in \Theta_h\}$. From (1), it follows that each discrete function $\mathbf{u}_h(\mathbf{x}') \in (l_h^2(G_h))^2$ can be written as a formal linear combination of the Fourier modes, which are linearly independent discrete functions.

Due to the fact that the grid and the frequency space are referred to as reciprocal bases, the Fourier modes have a formal expression, in terms of $\boldsymbol{\theta}''$ and \mathbf{x}' , similar to those in Cartesian coordinates. Therefore, the Local Fourier analysis on non-rectangular grids can be performed straightforwardly.

Let \mathcal{T}_h be a regular triangular grid on a fixed coarse triangle \mathcal{T} ; see left picture of Figure 2. \mathcal{T}_h is extended to the infinite grid G_h given before, where \mathbf{e}'_1 and \mathbf{e}'_2 are unit vectors indicating

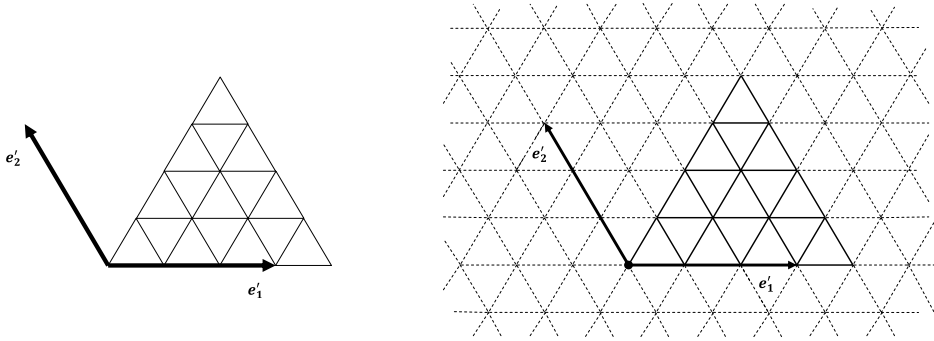


Figure 2: Regular triangular grid on a fixed coarse triangle \mathcal{T} and its extension to an infinite grid.

the direction of two of the edges of \mathcal{T} , and such that $\mathcal{T}_h = G_h \cap \mathcal{T}$, see right picture of Figure 2. Neglecting boundary conditions and/or connections with other neighboring triangles of the coarsest grid, the discrete problem $\mathbf{L}_h \mathbf{u}_h = \mathbf{f}_h$ can be extended to the whole grid G_h . As it is well-known, vector Fourier modes $\varphi_h(\boldsymbol{\theta}'', \mathbf{x}')$ are formal eigenfunctions of the discrete operator \mathbf{L}_h . More precisely, it is fulfilled

$$\mathbf{L}_h \varphi_h(\boldsymbol{\theta}'', \mathbf{x}') = \tilde{\mathbf{L}}_h(\boldsymbol{\theta}'') \varphi_h(\boldsymbol{\theta}'', \mathbf{x}'), \quad \tilde{\mathbf{L}}_h(\boldsymbol{\theta}'') = \begin{pmatrix} \tilde{L}_h^{u,u}(\boldsymbol{\theta}'') & \tilde{L}_h^{u,v}(\boldsymbol{\theta}'') \\ \tilde{L}_h^{v,u}(\boldsymbol{\theta}'') & \tilde{L}_h^{v,v}(\boldsymbol{\theta}'') \end{pmatrix},$$

where matrix $\tilde{\mathbf{L}}_h(\boldsymbol{\theta}'')$ is the Fourier symbol of \mathbf{L}_h .

Using standard coarsening, high and low frequency components on G_h are distinguished, in the way that the subset of low frequencies is $\Theta_{2h} = (-\pi/2h_1, \pi/2h_1] \times (-\pi/2h_2, \pi/2h_2]$, and the subset of high frequencies is $\Theta_h \setminus \Theta_{2h}$.

From these definitions LFA smoothing and two-grid analysis can be performed as in rectangular grids, and smoothing factors for the relaxing methods μ and two-grid convergence factors ρ , which give the asymptotic convergence behavior of the method, can be well defined.

§3. Relaxing methods

Collective three-color smoother and some collective line-wise smoothers are proposed as relaxing methods. These smoothers appear as a natural extension to triangular grids of some smoothers widely used on rectangular grids, as red-black Gauss-Seidel and line-wise relaxations of zebra type.

3.1. Three-color smoother

To apply three-color smoother, the grid associated with a fixed refinement level η of a triangle T of the coarsest triangulation,

$$G_{T,h} = \{\mathbf{x}' = (x'_1, x'_2) \mid x'_j = k_j h_j, k_j \in \mathbb{Z}, j = 1, 2, k_1 = 0, \dots, 2^\eta, k_2 = 0, \dots, k_1\}, \quad (2)$$

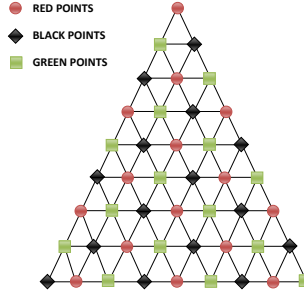


Figure 3: Three-color smoother.

is split into three disjoint subgrids,

$$G_{T,h}^i = \{\mathbf{x}' = (x'_1, x'_2) \in G_{T,h} \mid x'_j = k_j h_j, j = 1, 2, k_1 + k_2 = i \pmod{3}\}, \quad i = 0, 1, 2,$$

each of them associated with a different color, as shown in Figure 3, so that the unknowns of the same color have no direct connection with each other.

The complete three-color smoothing operator is given by the product of three partial operators, $\mathbf{S}_h(\omega) = \mathbf{S}_h^2(\omega)\mathbf{S}_h^1(\omega)\mathbf{S}_h^0(\omega)$. In each partial relaxation step, only the grid points of $G_{T,h}^i$ are processed, whereas the remaining points are not treated, i.e.

$$\mathbf{S}_h^i(\omega)\mathbf{v}_h(\mathbf{x}') = \begin{cases} [(\mathbf{I}_h - \omega\mathbf{D}_h^{-1}\mathbf{L}_h)\mathbf{v}_h](\mathbf{x}'), & \mathbf{x}' \in G_{T,h}^i, \\ \mathbf{v}_h(\mathbf{x}'), & \mathbf{x}' \in G_{T,h} \setminus G_{T,h}^i, \end{cases}$$

where \mathbf{D}_h is the diagonal part of the discrete operator \mathbf{L}_h , \mathbf{I}_h is the identity operator and ω is a relaxation parameter.

3.2. Zebra-type smoothers

For triangular grids, three different zebra smoothers can be defined on a triangle as shown in Figure 4. They consist of two half steps. In the first half-step, odd lines parallel to the edges of the triangle are processed, whereas even lines are relaxed in the second step, in which the updated approximations on the odd lines are used. They will be denoted as zebra-red, zebra-black and zebra-green smoothers, since they correspond to each of the vertices of the triangle.

In order to perform these smoothers, a splitting of the grid $G_{T,h}$ into two different subsets $G_{T,h}^{even}$ and $G_{T,h}^{odd}$ is necessary. For each of the zebra smoothers these subgrids are defined in a different way, and the corresponding distinction between them is specified in Table 1, where k_1 and k_2 are the indices of the grid points given in (2). Thus, these three smoothers \mathbf{S}_h^{zR} , \mathbf{S}_h^{zB} and \mathbf{S}_h^{zG} are defined by the product of two partial operators. For example, if zebra-red smoother is considered, $\mathbf{S}_h^{zR} = \mathbf{S}_h^{zR-even}\mathbf{S}_h^{zR-odd}$ where $\mathbf{S}_h^{zR-even}$ is in charge of relaxing the points in $G_{T,h}^{even}$ and \mathbf{S}_h^{zR-odd} is responsible for the points in $G_{T,h}^{odd}$. These smoothers are preferred to the

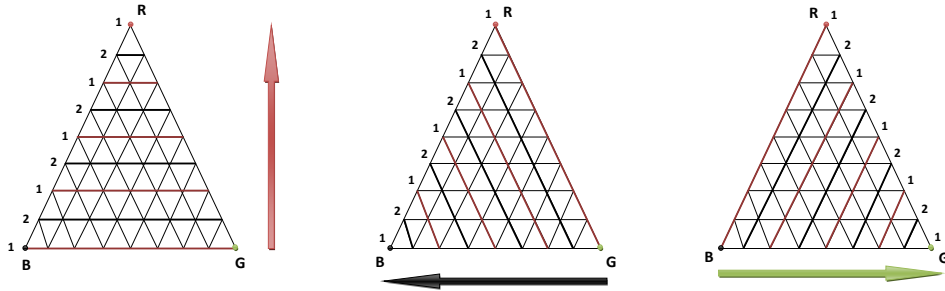


Figure 4: Zebra line smoothers: approximations at points marked by 1 are updated in the first half-step of the relaxation, and those marked by 2 in the second.

Relaxation	$G_{T,h}^{even}$	$G_{T,h}^{odd}$
Zebra-red	k_2 even	k_2 odd
Zebra-black	k_1 even	k_1 odd
Zebra-green	$k_1 + k_2$ even	$k_1 + k_2$ odd

Table 1: Characterization of subgrids $G_{T,h}^{even}$ and $G_{T,h}^{odd}$ for different zebra smoothers.

lexicographic line-wise Gauss-Seidel because in spite of having the same computational cost, smoothing factors corresponding to zebra smoothers are better than those of lexicographic line-wise relaxations as we will see further on.

§4. Fourier analysis results

It is easy to see that $\tilde{\mathbf{L}}_{R,h} = R \tilde{\mathbf{L}}_h R^t$, where $\tilde{\mathbf{L}}_h$ and $\tilde{\mathbf{L}}_{R,h}$ are the LFA symbols of the discrete operators associated with two grids, one obtained by rotating the other. Thus, it is fulfilled that these LFA symbols are similar and therefore LFA results obtained for these two grids are completely identical. Due to this property it is possible to restrict the analysis to triangles that sit on the x-axis of the Cartesian coordinate system.

This section focuses on analyzing different smoothers for the posed problem, while the components of the coarse-grid correction are taken as the standard ones as we have mentioned before.

One of the proposals here is the three-color smoother. In order to support the choice of this smoother as a good option for some geometries, some results obtained comparing it with the point-wise Gauss-Seidel are presented. For an equilateral triangle, these results appear in Table 2, where their two-grid convergence factors ρ and also the experimentally measured W-cycle convergence factors, denoted by ρ_h and obtained with a zero right-hand side and a random initial guess, are shown in order to observe that convergence factors are very well predicted by LFA. It can be observed that three-color smoother provides the best convergence factors between the two smoothers.

However, the three-color smoother is not robust over all angles, that is, the highly satis-

ν_1, ν_2	Gauss–Seidel		Three–color smoother	
	$\rho(\nu_1, \nu_2)$	$\rho_h(\nu_1, \nu_2)$	$\rho(\nu_1, \nu_2)$	$\rho_h(\nu_1, \nu_2)$
1, 0	0.516	0.506	0.422	0.422
1, 1	0.257	0.255	0.173	0.172
2, 1	0.172	0.172	0.097	0.095
2, 2	0.113	0.113	0.073	0.072

Table 2: Two–grid convergence factors ρ and measured W –cycle convergence rates ρ_h for equilateral triangles.

ν_1, ν_2	Equilateral		Isosceles (75°)		Isosceles (85°)	
	$\mu^{\nu_1+\nu_2}$	$\rho(\nu_1, \nu_2)$	$\mu^{\nu_1+\nu_2}$	$\rho(\nu_1, \nu_2)$	$\mu^{\nu_1+\nu_2}$	$\rho(\nu_1, \nu_2)$
1, 0	0.503	0.422	0.811	0.814	0.976	0.977
1, 1	0.253	0.173	0.657	0.661	0.954	0.955
2, 1	0.127	0.097	0.533	0.536	0.932	0.934
2, 2	0.064	0.073	0.432	0.435	0.911	0.913

Table 3: LFA smoothing and two–grid factors for different triangles with three-color smoother.

factory factors obtained for equilateral triangles worsen when one of the angles of the triangle is small. This behavior can be seen in Table 3, where smoothing and two-grid factors obtained with this smoother are shown for some representative triangles.

To overcome this difficulty, three zebra-type smoothers, associated with the three vertices of the triangle, are proposed. These zebra–type smoothers are preferred to the lexicographic block–line Gauss–Seidel smoothers because, despite having the same computational cost, they are more suitable for parallel implementation and their two-grid convergence factors are better, as we can see in Table 4 for an isosceles triangle with common angle 85°. Each of these zebra–type smoothers is highly efficient when the angle corresponding to the vertex of its color is sufficiently small. This is shown in Table 5, where smoothing and two-grid factors for some representative triangles are shown.

As a final remark, it is observed that, depending on the geometry of the triangles, it is possible to improve the convergence factors of three-color and zebra-type smoothers by means of a relaxation parameter, whereas for the point-wise Gauss-Seidel and lexicographic line-wise smoothers there is no improvement. For instance, in the case of equilateral triangles the obtained convergence factor for three-color smoother is about 0.422 for $\nu_1 = 1, \nu_2 = 0$, and it can enhance to 0.303 taking a damping parameter $\omega = 1.1$.

§5. Conclusions

A Local Fourier Analysis for multigrid methods on triangular grids for the problem of planar elasticity has been presented. Analogously to the scalar case, the key point of this analysis is to introduce an expression of the Fourier transform in new coordinate systems, both in space and in frequency variables, associated with reciprocal bases. This analysis makes highly

ν_1, ν_2	Lexicographic line-wise smoother		Zebra-type smoother	
	$\rho(\nu_1, \nu_2)$	$\rho_h(\nu_1, \nu_2)$	$\rho(\nu_1, \nu_2)$	$\rho_h(\nu_1, \nu_2)$
1, 0	0.333	0.331	0.143	0.142
1, 1	0.151	0.145	0.071	0.069
2, 1	0.094	0.094	0.047	0.046
2, 2	0.063	0.062	0.036	0.034

Table 4: LFA two-grid convergence factors and measured W -cycle convergence rates ρ_h for isosceles triangles with common angle 85° .

ν_1, ν_2	Equilateral		Isosceles (75°)		Isosceles (85°)	
	$\mu^{\nu_1+\nu_2}$	$\rho(\nu_1, \nu_2)$	$\mu^{\nu_1+\nu_2}$	$\rho(\nu_1, \nu_2)$	$\mu^{\nu_1+\nu_2}$	$\rho(\nu_1, \nu_2)$
1, 0	0.535	0.404	0.387	0.165	0.265	0.143
1, 1	0.226	0.164	0.096	0.072	0.053	0.071
2, 1	0.104	0.088	0.034	0.047	0.034	0.047
2, 2	0.049	0.067	0.025	0.035	0.025	0.036

Table 5: LFA smoothing and two-grid factors for equilateral and isosceles triangles with zebra-type smoother.

accurate predictions of the performance of a multigrid algorithm and as a consequence, also the choice of the adequate components of the method for a given problem. In this paper LFA has been applied to study the planar elasticity system, and with the help of this analysis a three-color smoother and some zebra-type smoothers are proposed to obtain an efficient multigrid algorithm to solve this problem.

Acknowledgements

This research has been partially supported by FEDER/MCYT Projects MTM2007-63204 and the DGA (Grupo consolidado PDIE).

References

- [1] BERGEN, B., GRADL, T., HÜLSEMANN, F., AND RÜDE, U. A massively parallel multigrid method for finite elements. *Comput. Sci. Eng.* 8 (2006), 56–62.
- [2] BRANDT, A. Multi-level adaptive solutions to boundary-value problems. *Comput. Sci. Eng.* 31 (1977), 333–390.
- [3] GASPAR, F. J., GRACIA, J. L., AND LISBONA, F. J. Fourier analysis for multigrid methods on triangular grids. *SIAM J. Sci. Comput.* 31 (2009), 2081–2102.
- [4] TROTTEBERG, U., OOSTERLEE, C. W., AND SCHÜLLER, A. *Multigrid*. Academic Press, New York, 2001.
- [5] WIENANDS, R., AND JOPPICH, W. *Practical Fourier analysis for multigrid methods*. Chapman and Hall/CRC Press, 2005.

F. J. Gaspar, J. L. Gracia, F. J. Lisbona and C. Rodrigo

Department of Applied Mathematics

University of Zaragoza

fjgaspar@unizar.es, jlgracia@unizar.es, lisbona@unizar.es and carmenr@unizar.es